



Cite this: *J. Anal. At. Spectrom.*, 2025, 40, 3210

Isobaric interference removal for selected radionuclides using nitrous oxide and ammonia with inductively coupled plasma tandem mass spectrometry

Shaun T. Lancaster, ^{*a} Ben Russell, ^b Thomas Prohaska ^{ac} and Johanna Irrgeher ^{ac}

The determination of long-lived radionuclides by inductively coupled plasma tandem mass spectrometry (ICP-MS/MS) is a well-established approach. However, such determinations can still be hindered by isobaric interferences from stable isotopes of neighbouring elements. As such, investigations towards novel gas cell approaches for removing interfering ions are required in order to improve the reliability of the analysis. Nitrous oxide (N₂O) is a reaction gas that has been well studied for stable isotope analysis. Studies towards its applicability to radionuclide analysis have so far been limited. Here, the use of N₂O, as well as a mixture with ammonia (NH₃), have been evaluated for determinations of 10 radionuclides of interest for nuclear decommissioning: ⁴¹Ca, ⁶³Ni, ⁷⁹Se, ⁹⁰Sr, ⁹³Zr, ⁹³Mo, ⁹⁴Nb, ¹⁰⁷Pd, ¹³⁵Cs, and ¹³⁷Cs. Single element solutions of stable isotope analogues of the radionuclides, as well as solutions of the interfering ions, were used to observe the reactions with the ICP-MS/MS reaction cell gases. Abundance-corrected sensitivities were used to assess the achievable separation factors and sensitivities for the determination of the radionuclides of interest. The N₂O/NH₃ gas mixture was found to provide a significant enhancement in the removal of isobaric interferences, as well as instrument detection limits (given in brackets), compared to N₂O alone for determinations of ⁴¹Ca (0.50 pg g⁻¹ (0.0016 Bq g⁻¹)), ⁷⁹Se (0.11 pg g⁻¹ (5.4 × 10⁻⁵ Bq g⁻¹)), ⁹⁰Sr (0.11 pg g⁻¹ (0.56 Bq g⁻¹)), ⁹³Mo (0.12 pg g⁻¹ (0.0044 Bq g⁻¹)), ¹³⁵Cs (0.1 pg g⁻¹ (7.5 × 10⁻⁶ Bq g⁻¹)), and ¹³⁷Cs (0.1 pg g⁻¹ (0.33 Bq g⁻¹)).

Received 30th June 2025
 Accepted 10th September 2025

DOI: 10.1039/d5ja00254k

rsc.li/jaas

^aDepartment of General, Analytical and Physical Chemistry, Chair of General and Analytical Chemistry, Montanuniversität Leoben, Leoben, Austria. E-mail: shaun.lancaster@unileoben.ac.at; johanna.irrgeher@unileoben.ac.at; thomas.prohaska@unileoben.ac.at

^bNuclear Metrology Group, National Physical Laboratory, Hampton Road, Teddington, UK. E-mail: ben.russell@npl.co.uk

^cDepartment of Physics and Astronomy, University of Calgary, Calgary, Canada



Shaun T. Lancaster

Shaun Lancaster currently holds a permanent position at Montanuniversität Leoben, Austria. He earned his PhD in 2021 in conjunction with the University of Aberdeen, Scotland, and instrument manufacturer P S Analytical, England. His work focused on method development for mercury speciation and subsequent analysis of methylmercury in the livers of Scottish birds of prey, as well as the development of novel atomic fluorescence based instrumentation for continuous monitoring of mercury in effluent wastewater streams. Following this, he began his postdoc at Montanuniversität Leoben working on the development of analytical methodology using ICP-MS/MS and XRF for the analysis of complex electronic waste matrices to assist the recycling industry as part of the drive towards a circular economy. Since taking a permanent position, his future ambition is to utilize ICP-MS/MS reaction cell gas chemistry to unlock new analytical approaches to solve challenging applications. In particular, to remove spectral interferences on difficult-to-measure isotopes for stable isotope ratio and radionuclide determinations, as well as for isotope ratio determinations of oxygen, which have previously never been performed by ICP-MS/MS.



Introduction

Decommissioning of nuclear sites represents a high cost and long-term analytical challenge to return the site to a safe state for future reactor development or alternative use. This necessitates the accurate measurement of a range of radionuclides in complex and varied sample matrices. Of particular interest are the medium and long-lived radionuclides that represent the most significant contribution to the long-term waste inventory that must be safely stored or disposed of. Examples include waste products generated from nuclear fission of ^{235}U , such as ^{79}Se , ^{90}Sr , ^{93}Zr , ^{107}Pd , ^{135}Cs , and ^{137}Cs , as well as activation products such as ^{41}Ca , ^{63}Ni , ^{93}Mo , and ^{94}Nb formed by neutron capture in the concrete and steel casings of the nuclear reactor.¹ Efficient characterisation of radioactive waste streams is key for safe and cost effective waste management, and requires the use of rapid and robust analytical methodology.

Inductively coupled plasma mass spectrometry (ICP-MS) has been for decades a frequently applied method of choice for the determination of long-lived radionuclides, providing more rapid analysis of samples compared to decay counting instrumentation and thereby contributing to faster and more cost-effective decommissioning.^{1,2} Accurate quantitative determinations of long-lived radionuclides by ICP-MS are hindered primarily by isobaric interferences from naturally occurring stable isotopes of other elements, as well as polyatomic ions and peak tailing interferences from neighbouring masses, often requiring time-consuming offline chromatographic separations to resolve. Modern quadrupole-based ICP-MS systems are equipped with a reaction cell that can be used to resolve isobaric interferences based on the differences in reactivity of different elements. Target analytes can be determined using either a mass-shift approach, where the analyte of interest is selectively reacted to form a product ion at a higher mass-to-charge ratio (m/z), or an on-mass approach, where the interfering ion is selectively reacted and the analyte of interest is measured without altering its m/z .³ With the advent of tandem mass spectrometry (MS/MS), only interferences at the m/z of the target analyte are of concern, as a quadrupole mass filter removes all other ions prior to entering the gas cell.⁴

The most commonly utilized cell gases for interference removal are hydrogen (H_2), helium (He), oxygen (O_2), and ammonia (NH_3).⁴ Of these, O_2 and NH_3 are commonly used for the removal of isobaric interferences for radionuclide determinations.^{5,6} Both H_2 and He have high ionisation energies and have low reactivity with most elements, and are typically employed as collisional gases, which can only reduce polyatomic interferences (by kinetic energy discrimination). Reactive cell gases can be combined with He to improve the interference separation. The addition of an unreactive gas can enhance sensitivity and reactions through the collisional focussing effect, focussing the ions to the minimum of the effective potential of the quadrupole by reducing the radial kinetic energy of the ion.^{7,8} Moreover, the addition of H_2 to NH_3 gas was observed to improve formation of $\text{M}(\text{NH}_3)_n$ product ions, rather than splitting the sensitivity between product ions with a lower number of hydrogen atoms,⁹ demonstrating that

combining two gases can lead to a different product ion formation. Uncovering new and improved interference removal pathways through ICP-MS/MS reaction cell chemistry can improve detection limits, sample throughput, and provide simpler methodology by minimizing the need for complex and time consuming chemical separations. Thus, further investigation into the use of alternative cell gases and cell gas combinations is necessary to expand options for end users.

Nitrous oxide (N_2O) is a reaction gas that has been extensively studied for stable isotope determinations,^{10–13} however for radionuclides its use has been limited primarily to the removal of radioactive caesium isotopes from stable barium isotopes enabling $^{135}\text{Cs}/^{137}\text{Cs}$ source attribution, which is a valuable tool for long-term environmental monitoring and used following the Fukushima disaster.^{14–16} Additionally, limited studies focus on mixtures of N_2O with other gases, such as He, H_2 and NH_3 .^{17,18} As such, this study aims to evaluate the use of N_2O , as well as gas mixtures of N_2O with NH_3 , as ICP-MS/MS cell gases for the removal of isobaric interferences on 10 radionuclides that are of importance in waste characterisation for nuclear decommissioning: ^{41}Ca , ^{63}Ni , ^{79}Se , ^{90}Sr , ^{93}Zr , ^{93}Mo , ^{94}Nb , ^{107}Pd , ^{135}Cs , and ^{137}Cs . To achieve this, elemental standards containing stable isotopes of the elements of interest were utilized as analogues to assess the reactivity of the elements compared to the reactivity of the isobaric interferences. Sensitivities and interference separation factors for the target radionuclides were calculated using the instrument response of the stable analogues and factoring the isotopic abundances.

Experimental

Reagents

Nitric acid (HNO_3 , $w = 65\%$, p.a. grade; Carl Roth GmbH, Karlsruhe, Germany) was purified using a sub-boiling distillation system (Savillex DST-4000, AHF Analysentechnik, Tübingen, Germany). Reagent grade I water ($18.2\text{ M}\Omega\text{ cm}$; MilliQ IQ 7000, Merck-Millipore, Darmstadt, Germany) was used for all acid dilutions. Vials and pipette tips were pre-cleaned by soaking overnight in diluted sub-boiled nitric acid ($w = 3\%$) before use.

Single-element standards of caesium (Cs), copper (Cu), potassium (K), magnesium (Mg), molybdenum (Mo) ($\beta = 1000\text{ }\mu\text{g mL}^{-1}$; Certipur, Merck); aluminium (Al), barium (Ba), calcium (Ca), iron (Fe), niobium (Nb), palladium (Pd), strontium (Sr), zirconium (Zr) ($\beta = 1000\text{ }\mu\text{g mL}^{-1}$; Inorganic Ventures, Christiansburg, VA, USA); ytterbium (Y, $\beta = 1000\text{ }\mu\text{g mL}^{-1}$; High Purity Standards, North Charleston, SC, USA); selenium (Se, $\beta = 1000\text{ }\mu\text{g mL}^{-1}$; Peak Performance, CPI international, Santa Rosa, CA, USA); nickel (Ni, $\beta = 1000\text{ }\mu\text{g mL}^{-1}$; Alfa Aesar, Karlsruhe, Germany); and silver (Ag, $\beta = 10\text{ }\mu\text{g mL}^{-1}$; Inorganic Ventures) were used throughout this work. Potassium bromide (NORMAPUR grade; VWR, Vienna, Austria) salt was used to prepare standards for the analysis of bromine (Br).

Instrumentation

All work was carried out using a NexION 5000 ICP-MS/MS system (PerkinElmer, Waltham, MA, USA) equipped with



Table 1 Operational parameters of the ICP-MS/MS system

Parameter	Standard mode	N ₂ O DRC mode	N ₂ O/NH ₃ DRC mode
Scan mode	MS/MS	MS/MS	MS/MS
Cell gas	None	N ₂ O	N ₂ O and NH ₃
RPa	0	0	0
RPq	0.25	0.45	0.45
Sample introduction	Self-aspiration	Self-aspiration	Self-aspiration
Nebulizer	PFA MicroFlow	PFA MicroFlow	PFA MicroFlow
Spray chamber	Peltier cooled SilQ cyclonic spray chamber	Peltier cooled SilQ cyclonic spray chamber	Peltier cooled SilQ cyclonic spray chamber
Spray chamber temperature	5 °C	5 °C	5 °C
Interface cones	Nickel	Nickel	Nickel
RF power	1600 W	1600 W	1600 W
Ar nebulizer gas flow	0.92–0.98 L min ⁻¹	0.92–0.98 L min ⁻¹	0.92–0.98 L min ⁻¹
Ar auxiliary gas flow	1.2 L min ⁻¹	1.2 L min ⁻¹	1.2 L min ⁻¹
Ar plasma gas flow	16 L min ⁻¹	16 L min ⁻¹	16 L min ⁻¹
Hyperskimmer park voltage	5 V	5 V	5 V
OmniRing park voltage	–185 V	–185 V	–185 V
Inner target lens voltage	2 V	2 V	2 V
Outer target lens voltage	–7 V	–7 V	–7 V
Deflector exit voltage	–8 V	–8 V	–8 V
Differential aperture voltage	–3.5 V	–3.5 V	–3.5 V
Q1 AC rod offset	–6 V	–10 V	–10 V
Q1 rod offset	–2 V	0 V	0 V
Cell rod offset	–33 V	–5 V	–5 V
Axial field voltage	0 V	250 V	250 V
Cell entrance voltage	–5 V	–8.5 V	–8.5 V
Cell exit voltage	–2 V	–5.5 V	–5.5 V
Q3 AC rod offset	–2.5 V	–7 V	–7 V
Q3 rod offset	–2 V	–10 V	–10 V
Dwell time	50 ms	50 ms	50 ms

a quadrupole-based dynamic reaction cell (DRC). The applied bandpass of the reaction cell quadrupole can be modified using rejection parameter “a” (RPa) and rejection parameter “q” (RPq). Instrument parameters for the different measurement modes applied are given in Table 1. Argon (purity 5.0 (≥99.999%); Linde Gas GmbH, Stadl-Paura, Austria) was used as the plasma gas. Nitrous oxide (medicinal grade; Linde Gas GmbH) and ammonia (purity 5.0 (≥99.999%); Linde Gas GmbH) were used as reaction gases.

Analytical measurement

Standards were diluted in nitric acid ($w = 2\%$). The isotopes of stable analogues and interferences monitored in this study are listed in Table 2. Initial mass scans were carried out using 0.8 mL min⁻¹ N₂O, as well as a mixture of 0.8 mL min⁻¹ N₂O and 0.4 mL min⁻¹ NH₃, in order to identify product ions that formed for each element monitored. Further investigation was carried out by varying gas flow rates and monitoring selected product ions.

Once the optimum gas flow rates had been determined for the removal of isobaric interferences, further interferences from elevated levels of Mg (as MgO), Al (as Al) and Fe (as ArFe) were assessed by introducing each interfering element as a 5 μg g⁻¹ single element standard and monitoring the instrument response.

Data processing. Sensitivities for radionuclides were determined from their stable analogues by scaling the isotopic abundances to 100% *via* eqn (1):

$$k_{\text{radionuclide}} = \frac{(I_{\text{std}} - I_{\text{blk}})}{w_{\text{std}}x} \quad (1)$$

where k is the sensitivity in cps (ng⁻¹ g⁻¹), I_{std} and I_{blk} are the measured signal intensities (in cps) of the standard and the blank respectively, w_{std} is the mass fraction of the standard in ng g⁻¹, and x is the isotopic abundance (as isotope amount fraction) as stated by the IUPAC Commission on Isotopic Abundances and Atomic Weights.²⁰

The separation factor between a target radionuclide and its interference is given as the ratio of the sensitivity of the target analyte to the sensitivity of the interference ($k_{\text{radionuclide}}/k_{\text{interference}}$). The greater the separation factor, the better resolved the radionuclide measurement is. For stable isotopes, the sensitivity is based on the elemental concentration.

Product ion formation has been calculated by the ratio of the sensitivity of the product ion of an element to the sensitivity of the same element achieved on-mass in the absence of a cell gas ($k_{\text{product ion}}/k_{\text{on-mass, no gas}}$) and expressed as a percentage.

Instrument detection limits were determined as three times the standard deviation of 10 replicate determinations of the blank signal (using $w = 2\%$ HNO₃), divided by the sensitivity of the radionuclide. The sensitivity was determined by performing a calibration using 7 standards of the stable isotopes of each given element at the optimum cell gas conditions. The sensitivity was normalized to 100% abundance of the isotope to determine the sensitivity of radionuclide determinations, as in eqn (1). The concentrations of the standards were: 1–1000 pg



Table 2 List of radionuclides of interest and the isotope of the stable analogue and interferences measured in this study. Half-lives of the radionuclides of interest were sourced from the atomic and nuclear database of the Decay Data Evaluation Project.¹⁹ Abundances for the interferences are given as the isotopic abundance of the interfering element.²⁰ Abundances for polyatomic interferences are given as the product of the isotopic abundances of the elements it contains

Radionuclide	Half-life (years)	Stable analogue monitored	Spectral interference	Interference abundance (%)
⁴¹ Ca	100 200 ± 1700	⁴⁴ Ca	⁴¹ K	6.73
			⁴⁰ Ar ¹ H	99.59
			⁴⁰ Ca tailing	96.94
⁶³ Ni	98.7 ± 2.4	⁶⁰ Ni	⁶³ Cu	69.17
⁷⁹ Se	356 000 ± 40 000	⁸² Se	⁷⁹ Br	50.69
⁹⁰ Sr	28.80 ± 0.70	⁸⁸ Sr	⁹⁰ Zr	51.45
⁹³ Mo	4000 ± 800	⁹⁴ Mo	⁸⁹ Y ¹ H	99.97
			⁹³ Nb	100
			⁹³ Zr	n/a
⁹³ Zr	1 610 000 ± 60 000	⁹⁴ Zr	⁹³ Nb	100
			⁹³ Mo	n/a
			⁹⁴ Zr	17.38
⁹⁴ Nb	20 040 ± 40	⁹³ Nb	⁹⁴ Mo	9.19
¹⁰⁷ Pd	6 500 000 ± 300 000	¹⁰⁵ Pd	¹⁰⁷ Ag	51.84
¹³⁵ Cs	1 330 000 ± 190 000	¹³³ Cs	¹³⁵ Ba	6.59
¹³⁷ Cs	30.018 ± 0.022	¹³³ Cs	¹³⁷ Ba	11.23

g^{-1} for Ni, Sr, Zr, Nb, Mo, Pd, and Cs, 10–10 000 pg g^{-1} for Se, and 100–100 000 pg g^{-1} for Ca (due to the low abundance of the ⁴⁴Ca isotope).

In order to convert the sensitivities and instrument detection limits from mass fractions to activities, the specific activity was calculated for each radionuclide *via* eqn (2):

$$a = \frac{\ln(2)N_A}{t_{1/2}m_a} \quad (2)$$

where a is the specific activity in Bq g^{-1} of pure substance, N_A is the Avogadro constant, $t_{1/2}$ is the half-life of the radionuclide, and m_a is the atomic mass of the radionuclide. The mass fraction units (in ng g^{-1}) were converted to units of activity, A (in Bq g^{-1} of sample), *via* eqn (3):

$$A = w \times a \times 10^{-9} \quad (3)$$

where the factor of 10^{-9} is included to convert between g (in Bq g^{-1}) and ng (in ng g^{-1}).

Results and discussion

Calcium-41

⁴¹Ca ($t_{1/2} = 1.002 \times 10^5$ years) is produced by neutron activation of ⁴⁰Ca (96.94% abundance) present in the concrete shield surrounding nuclear reactors, which makes up a considerable amount of waste during decommissioning. Determinations of ⁴¹Ca has primarily been carried out using liquid scintillation counting (LSC) and accelerator mass spectrometry (AMS) following chemical separations.^{21–23} Recently, the first determinations of ⁴¹Ca by ICP-MS/MS were conducted by *Russell et al.*,²⁴ where the authors suggests the use of an $\text{NH}_3/\text{H}_2/\text{He}$ gas mixture for interference removal. By this approach, ⁴¹Ca⁺ does not react with NH_3 or H_2 , while interferences of ⁴⁰Ar¹H⁺ and ⁴⁰Ar⁺ (from peak tailing) are removed by a charge transfer

reaction with NH_3 . The authors reported a detection limit of 99 pg g^{-1} (0.32 Bq g^{-1}) and a sensitivity of 3700 cps ($\text{ng}^{-1} \text{g}^{-1}$) (1150 cps (Bq g^{-1})) for ⁴¹Ca.²⁴ However, the major drawback of the NH_3/H_2 approach is that the stable ⁴¹K isotope also does not react with either gas, therefore ⁴¹Ca determinations are still subject to interferences in matrices containing high K levels. In literature, N_2O has previously been demonstrated to remove argon-based interferences, as well as interferences of K, by mass-shifting to the CaO^+ product ion.^{25,26} However, group 2 elements are known to also form hydroxide product ions with N_2O due to impurities in the cell gas,²⁶ therefore peak tailing of stable ⁴⁰Ca may still be problematic.

In this study, a mixture of N_2O and NH_3 were tested for determinations of the ⁴¹Ca. The addition of NH_3 to the N_2O generally caused group 2 elements to primarily form the hydroxide product ion (+17 amu) instead of the oxide product ion, while no product ion formation was observed for the group 1 elements. The argon interference is also removed effectively, as both N_2O and NH_3 react with Ar and ArH by charge transfer. For the determination of ⁴¹Ca using the ⁴¹Ca¹⁶O¹H⁺ product ion, the optimum gas mixture was found to be 0.4 mL min^{-1} N_2O and 0.2 mL min^{-1} NH_3 , achieving a sensitivity of 50 000 cps ($\text{ng}^{-1} \text{g}^{-1}$) (15 500 cps (Bq g^{-1})) for ⁴¹Ca (Table S1). This gas mixture allowed interferences from peak tailing of ⁴⁰Ca to be successfully removed, as the ⁴⁰Ca¹⁶O¹H₂⁺ product ion was not observed to form. This was in contrast to using N_2O alone and monitoring the ⁴¹Ca¹⁶O⁺ product ion ($m/z = 57$) as impurities in the N_2O gas caused a noticeable shift of ⁴⁰Ca⁺ to ⁴⁰Ca¹⁶O¹H⁺ ($m/z = 57$). Importantly, the interference from ⁴¹K⁺ was eliminated due to the selective reaction of ⁴¹Ca⁺, thus providing a distinct advantage over the current best available methodology. The instrument detection limit achieved for ⁴¹Ca using the $\text{N}_2\text{O}/\text{NH}_3$ gas mixture approach was 0.35 pg g^{-1} (0.0011 Bq g^{-1}). Further investigation was also carried out to investigate the



effectiveness of the optimised $\text{N}_2\text{O}/\text{NH}_3$ gas mixture approach for sample matrices that may contain high levels of Mg, as $^{25}\text{Mg}^{16}\text{O}^+$ is an additional interference at m/z 41. Analysis of a $5 \mu\text{g g}^{-1}$ Mg standard indicated a minor interference of 17 cps ($\mu\text{g}^{-1} \text{g}^{-1}$) Mg. Thus samples with excessive Mg levels may require dilution.

Nickel-59/63. Neutron activation of stable Ni isotopes in steel reactor casings produce two long-lived Ni radionuclides: ^{59}Ni ($t_{1/2} = 7.6 \times 10^4$ years) and ^{63}Ni ($t_{1/2} = 98.7$ years). Following chemical separations, ^{63}Ni can be easily measured using LSC.^{27,28} The ^{59}Ni radionuclide is more challenging to measure by LSC due to the more abundant beta emissions of ^{63}Ni , but has been measured using X-ray emission techniques.²⁹ For ICP-MS/MS analysis, the ^{59}Ni and ^{63}Ni radionuclide have isobaric interferences from stable ^{59}Co and ^{63}Cu isotope, respectively. Russell *et al.*³⁰ demonstrated previously that an $\text{NH}_3/\text{H}_2/\text{He}$ gas mixture can be used to separate ^{63}Ni from the ^{63}Cu isobar. By this approach, ^{63}Ni reacts to form the $^{63}\text{Ni}(\text{NH}_3)_3^+$ product ion at a greater rate than the formation of $^{63}\text{Cu}(\text{NH}_3)_3^+$, achieving a $^{63}\text{Ni}/^{63}\text{Cu}$ separation factor of 100 and detection limits of 0.25 pg g^{-1} (0.52 Bq g^{-1}). The addition of H_2 to the NH_3/He mixture allowed for greater formation of the $\text{M}(\text{NH}_3)_n$ product ions. The authors additionally noted that the use of H_2 significantly improved the formation rate of the $^{63}\text{Ni}(\text{NH}_3)_3^+$ product ion, and reported an achieved sensitivity of $6100 \text{ cps (ng}^{-1} \text{g}^{-1})$ ($2.86 \text{ cps (Bq g}^{-1})$).

To date, there has been no successful ICP-MS/MS reaction cell based separation of ^{59}Ni from ^{59}Co reported in literature. While determinations of ^{59}Ni using N_2O and a $\text{N}_2\text{O}/\text{NH}_3$ gas mixture were attempted in this study, it was found that Co and Ni behaved very similarly under both conditions. As such, no separation of ^{59}Ni and ^{59}Co could be achieved and ^{59}Ni was not investigated further here.

Although Ni and Cu are both relatively unreactive with N_2O , minor formation of oxide product ions have been previously observed.¹³ In this study, Ni and Cu formed oxide product ions (+16 amu) at 4.6% and 0.1% respectively, allowing for a potential interference separation route. The maximum separation factor of 13 600 was achieved using a N_2O flow rate of 1.4 mL min^{-1} , achieving a ^{63}Ni sensitivity of $3640 \text{ cps (ng}^{-1} \text{g}^{-1})$ ($1.71 \text{ cps (Bq g}^{-1})$). The obtained instrument detection limit using N_2O was calculated to be 0.29 pg g^{-1} (0.62 Bq g^{-1}). Slightly higher sensitivities could be achieved by reducing the N_2O flow rate, but result in a less efficient separation of ^{63}Cu from ^{63}Ni (Fig. 1). For example, applying $1 \text{ mL min}^{-1} \text{ N}_2\text{O}$ achieved a ^{63}Ni sensitivity of $5310 \text{ cps (ng}^{-1} \text{g}^{-1})$ ($2.49 \text{ cps (Bq g}^{-1})$) and an instrument detection limit of 0.20 pg g^{-1} (0.42 Bq g^{-1}), but a lower separation factor of 4960. Despite the slightly lower sensitivity and higher instrument detection limits obtained compared to the existing $\text{NH}_3/\text{H}_2/\text{He}$ approach, the factor of 10 to 100 times greater separation factors achieved using N_2O provides a significant advantage. Moreover, samples containing elevated levels of Al may pose an additional challenge, as $^{36}\text{Ar}^{27}\text{Al}^+$ interferes on m/z 63 and, in this study, was observed to form at a rate of $11\,100 \text{ cps (}\mu\text{g}^{-1} \text{g}^{-1})$ Al in the absence of a cell gas. When applying N_2O at the optimum conditions, the rate of interference became negligible at $<0.1 \text{ cps (}\mu\text{g}^{-1} \text{g}^{-1})$ Al.

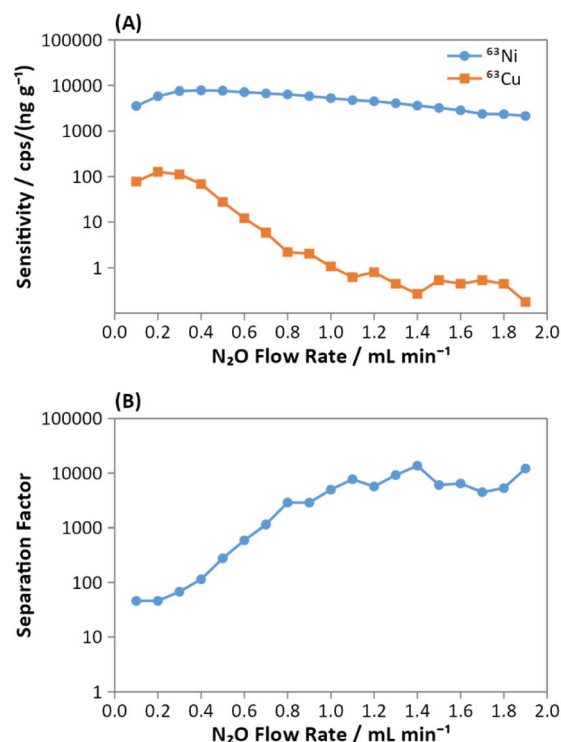


Fig. 1 (A) Calculated sensitivity of the ^{63}Ni radionuclide determined as the $^{63}\text{Ni}^{16}\text{O}^+$ product ion (blue, circle) and the obtained sensitivity of the $^{63}\text{Cu}^{16}\text{O}^+$ product ion (orange, square), and (B) the separation factor of $^{63}\text{Ni}/^{63}\text{Cu}$.

When applying an $\text{N}_2\text{O}/\text{NH}_3$ gas mixture, both Cu and Ni were observed to form product ions at +17 amu, +34 amu, and +51 amu (Fig. 2). While these 17 amu increments could correspond to either $^{16}\text{O}^1\text{H}$ or $^{14}\text{N}^1\text{H}_3$ ligands, it is likely that the $^{14}\text{N}^1\text{H}_3$ is forming, as the product ion formation rates aligned with previous literature using only NH_3 as a cell gas.³¹ Cu formed the $\text{Cu}(\text{NH}_3)_2^+$ at the highest rate (maximum of 7.4% at $0.4 \text{ mL min}^{-1} \text{ N}_2\text{O}$ and $1.0 \text{ mL min}^{-1} \text{ NH}_3$), while Ni was observed to form $\text{Ni}(\text{NH}_3)_3^+$ at the highest rate (maximum of 4.4% at $0.2 \text{ mL min}^{-1} \text{ N}_2\text{O}$ and $1.0 \text{ mL min}^{-1} \text{ NH}_3$). By utilizing the $\text{Ni}(\text{NH}_3)_3^+$ product ion with a gas mixture of $0.6 \text{ mL min}^{-1} \text{ N}_2\text{O}$ and $0.4 \text{ mL min}^{-1} \text{ NH}_3$, a similar sensitivity of $3440 \text{ cps (ng}^{-1} \text{g}^{-1})$ (equivalent to $1.62 \text{ cps (Bq g}^{-1})$) could be achieved, however with a separation factor of 254 (Table S2) – approximately 50 times less efficient than when using N_2O alone. Moreover, at these flow rates, slightly higher instrument detection limits of 0.58 ng g^{-1} (1.2 Bq g^{-1}) were obtained, and the removal of the $^{36}\text{Ar}^{27}\text{Al}^+$ interference was less efficient ($1.9 \text{ cps (}\mu\text{g}^{-1} \text{g}^{-1})$ Al) than when using N_2O alone. Hence, it would be recommended that the N_2O approach would be optimal for determinations of ^{63}Ni .

Selenium-79

^{79}Se ($t_{1/2} = 7.6 \times 10^4$ years) is a product of ^{235}U fission that is important to characterise during decommissioning due to its high environmental mobility. Given its long half-life, ICP-MS is well suited to the determination of the ^{79}Se radioisotope. In



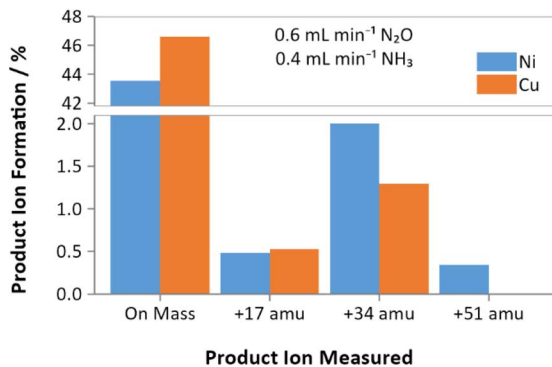


Fig. 2 Product ion formations of Ni (blue) and Cu (orange) with $0.6 \text{ mL min}^{-1} \text{ N}_2\text{O}$ and $0.4 \text{ mL min}^{-1} \text{ NH}_3$ applied as a reaction gas mixture.

addition to isobaric interferences from the stable ^{79}Br isotope, argon-based polyatomic interferences ($^{40}\text{Ar}^{38}\text{Ar}^1\text{H}^+$, $^{38}\text{Ar}_2^1\text{H}^+$, and peak tailing of $^{40}\text{Ar}_2^+$) present an additional challenge for the analysis of ^{79}Se by ICP-MS/MS. A recent publication utilized NH_3 gas with ICP-MS/MS to reduce ^{79}Br and argon-based interferences by charge transfer, following a chemical separation step. The authors achieved an instrument limit of detection of 1.2 pg mL^{-1} ($5.7 \times 10^{-4} \text{ Bq mL}^{-1}$).³² The authors additionally reported a separation factor of 7 orders of magnitude using their combined chemical separation and ICP-MS/MS methodology.

Here, bromine was observed to react very efficiently with N_2O to form the BrO^+ product ion, with a maximum product ion formation of 77% at 0.6 mL min^{-1} . Selenium was observed to react with N_2O to form the SeO^+ product ion, however the maximum product ion formation was 25% at a cell gas flow rate of 1.8 mL min^{-1} . At lower flow rates, the Se signal remained primarily on-mass, with a maximum of 96% signal intensity (relative to no cell gas) at an N_2O flow rate of 0.6 mL min^{-1} . By utilizing the on-mass determination of Se, separation of ^{79}Se from the interfering ^{79}Br can be achieved. A separation factor of 188 000 was achieved in this study using $2.0 \text{ mL min}^{-1} \text{ N}_2\text{O}$, with a calculated sensitivity for ^{79}Se of $3140 \text{ cps (ng}^{-1} \text{ g}^{-1})$ ($6670 \text{ cps (Bq g}^{-1})$) (Fig. 3), with instrument detection limits of 0.51 pg g^{-1} ($2.4 \times 10^{-4} \text{ Bq g}^{-1}$). Higher sensitivities could be achieved by reducing the N_2O flow rate, although at the cost of less efficient ^{79}Br interference removal. The argon-based polyatomic interferences were no longer observed at N_2O flow rates of 1.2 mL min^{-1} and above. At 1.2 mL min^{-1} , the ^{79}Se sensitivity obtained was $7520 \text{ cps (ng}^{-1} \text{ g}^{-1})$ ($16000 \text{ cps (Bq g}^{-1})$), with an instrument detection limit of 0.38 pg g^{-1} ($1.8 \times 10^{-4} \text{ Bq g}^{-1}$). Thus, the use of N_2O provides an alternative cell-gas approach to the recently developed NH_3 approach.

Applying the $\text{N}_2\text{O}/\text{NH}_3$ gas mixture improved interference removal at lower flow rates, allowing for determinations of ^{79}Se at greater sensitivities. By applying $0.4 \text{ mL min}^{-1} \text{ N}_2\text{O}$ and $0.2 \text{ mL min}^{-1} \text{ NH}_3$, a calculated sensitivity of $13100 \text{ cps (ng}^{-1} \text{ g}^{-1})$ (equivalent to $27800 \text{ cps (Bq g}^{-1})$) was achieved with an improved interference separation factor of 4 600 000 (Table S3)

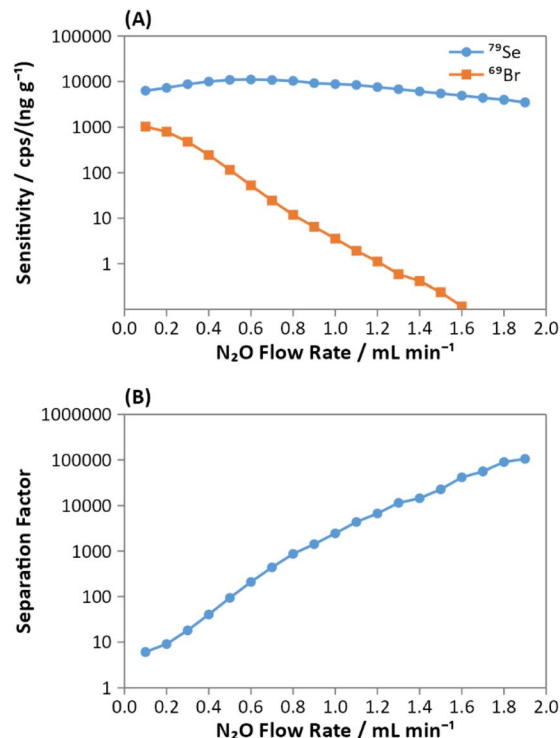


Fig. 3 (A) Calculated sensitivity of the ^{79}Se radionuclide determined on-mass (blue, circle) and the obtained sensitivity of the ^{79}Br interference determined on-mass (orange, square), and (B) the separation factor of $^{79}\text{Se}/^{79}\text{Br}$.

and a calculated instrument detection limit of 0.17 pg g^{-1} ($8.0 \times 10^{-5} \text{ Bq g}^{-1}$). This is likely due to an efficient charge transfer reaction between $^{79}\text{Br}^+$ and NH_3 . The use of NH_3 has been shown impede the sensitivity of Se at higher flow rates (by a charge transfer reaction).³³ In this case however, the low flow of NH_3 enhanced the removal of the ^{79}Br interference, but was not a high enough flow to impact the sensitivity of ^{79}Se . Moreover, it is possible that the N_2O acts to enhance the sensitivity of ^{79}Se on-mass through the collisional focussing effect.¹³ Therefore, the use of the $\text{N}_2\text{O}/\text{NH}_3$ mixture offers an alternative approach for improved sensitivity and lower instrument detection limits, as well as a high interference separation factor of 6–7 orders of magnitude that can compete with the chemical separation approaches.

Strontium-90

Another fission product of high concern is ^{90}Sr ($t_{1/2} = 28.80$ years), which is also known to be mobile in nature. Although this radionuclide can be determined using LSC following chemical separation,³⁴ ICP-MS determinations are growing more common due to advances in instrument sensitivity. The standard approach for interference removal for ^{90}Sr determinations by ICP-MS or ICP-MS/MS is the use of oxygen as a reaction gas.^{35,36} In this approach, oxygen reacts efficiently with the interfering $^{90}\text{Zr}^+$ (forming $^{90}\text{Zr}^{16}\text{O}^+$ and $^{90}\text{Zr}^{16}\text{O}_2^+$), as well as $^{89}\text{Y}^1\text{H}^+$, but does not react efficiently with ^{90}Sr , thus



allowing for an on-mass determination of ^{90}Sr . This established method is reported to provide instrument detection limits of 4 fg g^{-1} (0.02 Bq g^{-1}).³⁶

The use of N_2O provided separation of ^{90}Sr from $^{89}\text{Y}^+\text{H}^+$ interference by forming the $^{90}\text{Sr}^{16}\text{O}^+$ product ion ($m/z = 106$), with the $^{89}\text{Y}^{16}\text{O}^+\text{H}^+$ interference forming at $<0.3 \text{ cps (ng}^{-1} \text{ g}^{-1})$ (of ^{89}Y). However, the ^{90}Zr interference also reacted with N_2O to form $^{90}\text{Zr}^{16}\text{O}^+$. Higher flow rates of N_2O lead to a higher separation of ^{90}Sr from ^{90}Zr , however at the cost of lower sensitivity (Fig. 4). Using only N_2O , the maximum achieved separation factor for the removal of ^{90}Zr on ^{90}Sr was 10 600 at 3 mL min^{-1} , with a sensitivity of $2870 \text{ cps (ng}^{-1} \text{ g}^{-1})$ (equivalent to $0.562 \text{ cps (Bq g}^{-1})$) for ^{90}Sr . The instrument detection limit under these conditions was calculated to be 0.27 pg g^{-1} (equivalent to 1.4 Bq g^{-1}), which does not provide an advantage over the current best available methodology.

Applying an $\text{N}_2\text{O}/\text{NH}_3$ gas mixture and using the $^{90}\text{Sr}^{16}\text{O}^+\text{H}^+$ product ion ($m/z = 107$) provided a much greater separation from ^{90}Zr , with $<0.01\%$ product ion formation of Zr at $+17 \text{ amu}$. The maximum separation factor of 334 000 was achieved at gas flow rates of $0.8 \text{ mL min}^{-1} \text{ N}_2\text{O}$ and $0.5 \text{ mL min}^{-1} \text{ NH}_3$ (Table S4). Product ion scans indicated that Zr preferentially formed higher-order product ions (primarily at $+82 \text{ amu}$ to $+84 \text{ amu}$) using the $\text{N}_2\text{O}/\text{NH}_3$ gas mixture, allowing for more effective removal on $m/z 107$. Moreover, interferences from polyatomic $^{89}\text{Y}^+\text{H}^+$ and peak tailing of $^{89}\text{Y}^+$ were observed to be more effectively reduced using the $\text{N}_2\text{O}/\text{NH}_3$ gas mixture. By reducing

the NH_3 flow rate to 0.2 mL min^{-1} and maintaining a N_2O flow rate of 0.8 mL min^{-1} , a sensitivity of $108\,000 \text{ cps (ng}^{-1} \text{ g}^{-1})$ (equivalent to $21.1 \text{ cps (Bq g}^{-1})$) for ^{90}Sr was obtained (SrOH product ion formation of 38%), while the $^{90}\text{Sr}/^{90}\text{Zr}$ separation factor remained $>100\,000$ (Table S4), giving a much greater performance than using N_2O alone. The instrument detection limit for ^{90}Sr at these gas flow rates was calculated to be 0.015 pg g^{-1} (0.076 Bq g^{-1}), which is similar to the detection limits achieved by the oxygen cell gas approach^{35,36} and thus makes the $\text{N}_2\text{O}/\text{NH}_3$ gas mixture approach a viable alternative for interference removal.

Zirconium-93, molybdenum-93, and niobium-94

^{93}Zr ($t_{1/2} = 1.61 \times 10^6$ years), ^{93}Mo ($t_{1/2} = 4000$ years), and ^{94}Nb ($t_{1/2} = 2.004 \times 10^4$ years) are produced through neutron activation of stable ^{92}Zr (17.16% abundance), ^{92}Mo (14.65% abundance), and ^{93}Nb (100% abundance), respectively, that are contained within steel casings of nuclear reactors. Additionally, ^{93}Zr is also a high-yield fission product in spent nuclear fuel. Following chemical separations, ^{93}Zr and ^{93}Mo can be determined by LSC,^{37,38} whereas ^{94}Nb can be determined by gamma- or X-ray spectrometry.³⁹ Given the long half-lives, ICP-MS determinations are well suited to the analysis of these radionuclides. However, ^{93}Zr and ^{93}Mo share isobars with each other as well as ^{93}Nb , which provides an additional challenge as ^{93}Nb is the only stable isotope of Nb. ICP-MS/MS has previously been demonstrated to be an effective approach to analysing ^{93}Zr and ^{93}Mo . Petrov *et al.*⁹ reported that an $\text{NH}_3/\text{H}_2/\text{He}$ gas mixture could be utilized to effectively remove interferences of ^{93}Mo and ^{93}Nb on ^{93}Zr by measuring the $^{93}\text{Zr}(\text{NH}_3)_6$ product ion, with separation factors of 10^5 achievable from both interferences. The authors report a sensitivity of approximately $20\,000 \text{ cps (ng}^{-1} \text{ g}^{-1})$ ($230\,000 \text{ cps (Bq g}^{-1})$) and a detection limit of 0.14 pg g^{-1} ($1.3 \times 10^{-5} \text{ Bq g}^{-1}$) for ^{93}Zr . Russell *et al.*³⁰ subsequently demonstrated that the same $\text{NH}_3/\text{H}_2/\text{He}$ gas mixture could be utilized to analyse ^{93}Mo using the $^{93}\text{Mo}(\text{NH}_3)_2$ product ion. The authors reported a sensitivity of $1100 \text{ cps (ng}^{-1} \text{ g}^{-1})$ ($31 \text{ cps (Bq g}^{-1})$) and a detection limit of 45.6 pg g^{-1} (1.6 Bq g^{-1}). The ^{94}Nb radionuclide has been much less studied using ICP-MS/MS compared to ^{93}Zr and ^{93}Mo and, to the authors knowledge, there is no literature on the best available reaction gas conditions. Nevertheless, as the ^{94}Nb radionuclide shares isobars with stable ^{94}Zr and ^{94}Mo isotopes, it has also been assessed using N_2O and a $\text{N}_2\text{O}/\text{NH}_3$ gas mixture in this study.

Zr and Nb react with N_2O to form primarily oxide ($+16 \text{ amu}$) and dioxide ($+32 \text{ amu}$) product ions, whereas Mo reacts very little with N_2O .¹³ Therefore, the removal of stable ^{93}Nb interference, as well as interferences from the ^{93}Zr radionuclide, using an on-mass determination of ^{93}Mo would be possible. Using a flow rate of $1 \text{ mL min}^{-1} \text{ N}_2\text{O}$, ^{93}Mo could be separated from ^{93}Nb and ^{93}Zr by factors of 750 and 1160 respectively, while providing a calculated sensitivity of $126\,000 \text{ cps (ng}^{-1} \text{ g}^{-1})$ (equivalent to $3540 \text{ cps (Bq g}^{-1})$) (Fig. 5). The instrument detection limit was calculated to be 0.017 pg g^{-1} ($6.1 \times 10^{-4} \text{ Bq g}^{-1}$). Additionally, the ^{93}Zr and ^{94}Nb radionuclides can be

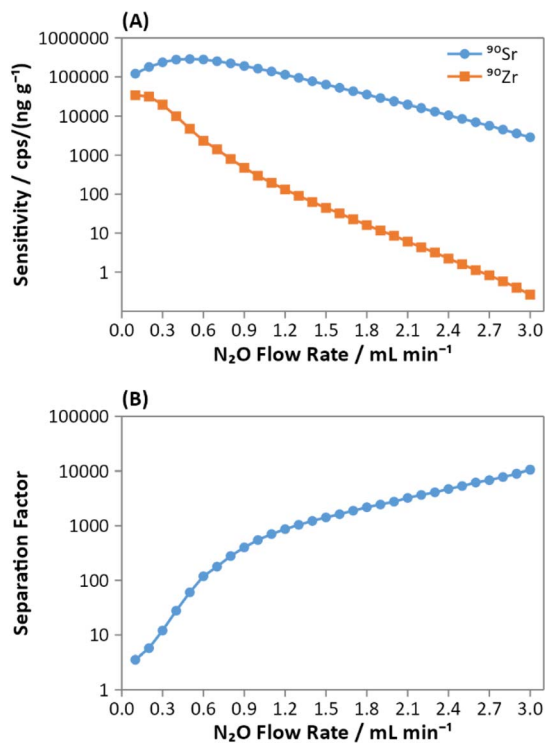


Fig. 4 (A) Calculated sensitivity of the ^{90}Sr radionuclide determined as the $^{90}\text{Sr}^{16}\text{O}^+$ product ion (blue, circle) and the obtained sensitivity of the ^{90}Zr interference determined as the $^{90}\text{Sr}^{16}\text{O}^+$ product ion (orange, square), and (B) the separation factor of $^{90}\text{Sr}/^{90}\text{Zr}$.



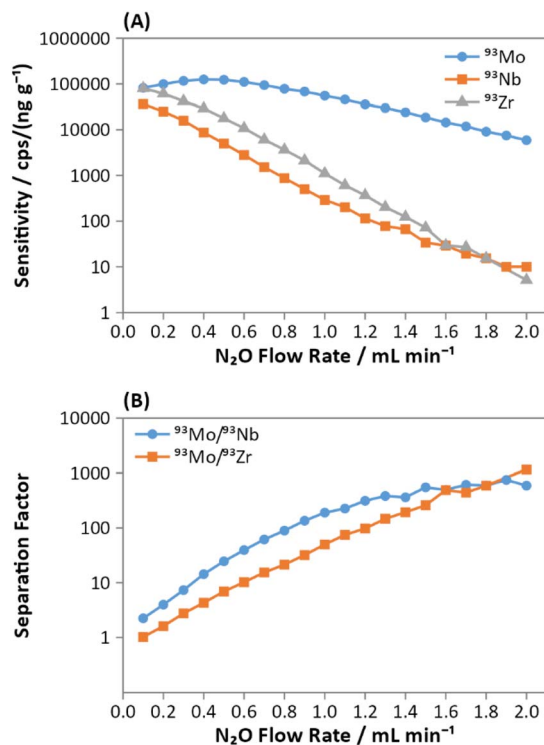


Fig. 5 (A) Calculated sensitivity of the ⁹³Mo radionuclide (blue, circle), the calculated sensitivity of the interfering ⁹³Zr radionuclide (grey, triangle) and the obtained sensitivity of the stable ⁹³Nb interference (orange, square), and (B) the separation factor of ⁹³Mo/⁹³Nb (blue, circle) and ⁹³Mo/⁹³Zr (orange, square).

separated from the ⁹³Mo radioisotope and the stable ⁹⁴Mo isotope respectively by mass-shifting and analysing the dioxide product ion. However, as Zr and Nb react very similarly with N₂O,¹³ these radionuclides cannot be separated from their stable isotope counterparts.

Applying an N₂O/NH₃ gas mixture, Mo was, again, found to react relatively little with the cell gas and most of the ions were transmitted on-mass. The Mo(OH)₂ product ion was formed at the highest rate (maximum of 3.2% formation). Nb and Zr preferentially reacted to form higher order product ions, primarily around +82 amu to +84 amu (Fig. 6). Both ¹⁴N¹H₃ and ¹⁶O¹H shift the mass by +17 amu, and can form ligands with and without the hydrogen atoms present (*i.e.* as MO⁺ or MNH₂⁺), therefore it is difficult to predict exactly which higher-order complexes are being formed at these higher masses. Nevertheless, the distinct differences in reactivity between Mo and the interfering Nb and Zr isobars mean that separation is possible. However, the addition of NH₃ resulted in a slightly lower sensitivity. Using 0.6 mL min⁻¹ N₂O and 0.4 mL min⁻¹ NH₃ achieved equivalent separation factors compared to using 1 mL min⁻¹ N₂O, with a calculated sensitivity for ⁹³Mo of 105 000 cps (ng⁻¹ g⁻¹) (equivalent to 2950 cps (Bq g⁻¹)) (Table S5), 17% lower than using N₂O alone. However, the instrument detection limit was calculated to be 0.015 pg g⁻¹ (5.5 × 10⁻⁴ Bq g⁻¹), which was similar to that obtained by using N₂O alone. Further improvements to the removal of Zr and Nb could be

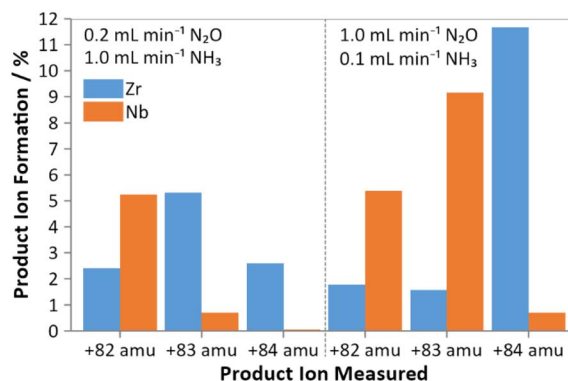


Fig. 6 Product ion formations of Zr (blue) and Nb (orange) under two different reaction gas mixtures: 0.2 mL min⁻¹ N₂O and 1.0 mL min⁻¹ NH₃ (left); and 1.0 mL min⁻¹ N₂O and 0.2 mL min⁻¹ NH₃ (right).

achieved by varying the N₂O and NH₃ flow rates, but at the cost of lower sensitivities for ⁹³Mo (Table S5).

Separation of Zr and Nb was found to be possible using the N₂O/NH₃ mixture, however with low separation factors. The product ions of Nb and Zr at +82 amu and +84 amu were found to form at different rates depending on the composition of the N₂O/NH₃ mixture. For ⁹³Zr, the greatest separation factor achieved for the removal of ⁹³Nb was 80 by observing the product ion at +84 amu and using a cell gas mixture of 0.2 mL min⁻¹ N₂O and 1 mL min⁻¹ NH₃ (Table S6). The high ammonia gas flow rate resulted in a relatively low sensitivity of 7670 cps (ng⁻¹ g⁻¹) (86 700 cps (Bq g⁻¹)), equivalent to 2.6% product ion formation. The instrument detection limit for ⁹³Zr was calculated to be 0.27 pg g⁻¹ (2.4 × 10⁻⁵ Bq g⁻¹). For ⁹⁴Nb, the greatest separation factor achieved for the removal of ⁹⁴Zr was 25 by observing the product ion at +83 amu and using 1 mL min⁻¹ N₂O and 0.1 mL min⁻¹ NH₃ (Table S7). In this case, the flow rates also corresponded to the maximum observed product ion formation of 9.6%, equivalent to a sensitivity of 19 900 cps (ng⁻¹ g⁻¹) (2830 cps (Bq g⁻¹)) for ⁹⁴Nb. The instrument detection limit for ⁹⁴Nb was calculated to be 0.23 pg g⁻¹ (0.0016 Bq g⁻¹). An additional concern for determinations of ⁹⁴Nb is the ⁴⁰Ar⁵⁴Fe⁺ interference in samples with elevated Fe content. In the absence of a cell gas, the interference formed at a rate of 82 cps (μg⁻¹ g⁻¹) Fe. At the flow rates of 1 mL min⁻¹ N₂O and 0.1 mL min⁻¹ NH₃, the interference was reduced to 0.7 cps (μg⁻¹ g⁻¹) Fe. However, given the low separation factors and sensitivity achieved for ⁹³Zr and ⁹⁴Nb, the use of the N₂O/NH₃ gas mixture may have limited application for these radionuclides.

Palladium-107

¹⁰⁷Pd (*t*_{1/2} = 6.5 × 10⁶ years) is a fission product found in spent nuclear fuel. Determinations by LSC are possible for ¹⁰⁷Pd, however given its very long half-life, ICP-MS determinations provide greater sensitivity compared to radiometric techniques.⁴⁰ For ICP-MS determinations, the radionuclide ¹⁰⁷Pd shares isobaric interferences with stable ¹⁰⁷Ag. Literature utilizing reaction gases for interference separation of ¹⁰⁷Pd is



limited, with studies focussing on improving chemical separations prior to ICP-MS detection.⁴¹ In combination with chemical separation, Weller *et al.*⁴⁰ utilized a propane/He gas mixture to separate ¹⁰⁷Pd from its isobaric interference by monitoring the Pd(C₂H₂) product ion, resulting in detection limits of <2 pg g⁻¹ (<4 × 10⁻⁵ Bq g⁻¹). The product ion formation was reported to be approximately 4%, which limits the available sensitivity, however the authors also report that similar detection limits were achieved for ¹⁰⁷Pd in the absence of a reaction gas.

Both Pd and Ag react very little with N₂O, with less than 1% product ion formation.¹³ However, Ag does not form AgO⁺ product ions (instead, favouring AgN₂O⁺ formation), whereas Pd does form PdO⁺ product ions.¹³ Therefore, determinations of the ¹⁰⁷Pd radionuclide may be possible. However, in this study, the maximum formation rate of the PdO⁺ product ion was 0.15% at 0.7 mL min⁻¹ N₂O, equating to a sensitivity of 164 cps (ng⁻¹ g⁻¹) (8620 cps (Bq g⁻¹)) for ¹⁰⁷Pd. The calculated instrument detection limit was 14 pg g⁻¹ (2.7 × 10⁻⁴ Bq g⁻¹). N₂O shows potentially limited use for determinations of ¹⁰⁷Pd due to the low achievable sensitivities.

Applying the N₂O/NH₃ gas mixture, Pd and Ag reacted to form product ions at +17 amu, +34 amu, and +51 amu. While these 17 amu increments could correspond to either ¹⁶O¹H or ¹⁴N¹H₃ ligands, it is likely that the ¹⁴N¹H₃ is forming, as the product ion formation rates aligned with previous literature using only NH₃ as a cell gas.³¹ The Ag(NH₃)₃⁺ product ion formed at a lower rate than that of Pd(NH₃)₃⁺. Using cell gas flow rates of 0.6 mL min⁻¹ N₂O and 0.8 mL min⁻¹ NH₃, a separation factor of 84 could be achieved, with a sensitivity of 3300 cps (ng⁻¹ g⁻¹) (173 000 cps (Bq g⁻¹)) (Table S8 and Fig. 7). The calculated instrument detection limit under these gas conditions was 1.1 pg g⁻¹ (2.0 × 10⁻⁵ Bq g⁻¹). While the achieved sensitivity is 20 times greater than using N₂O alone, the use of N₂O alone achieved detection of ¹⁰⁷Pd (as PdO⁺) free from ¹⁰⁷Ag interference, since the AgO⁺ product ion was not formed. Therefore, depending on the mass fraction of Ag present in the matrix, it may be preferable to use the N₂O approach over the N₂O/NH₃ gas mixture approach.

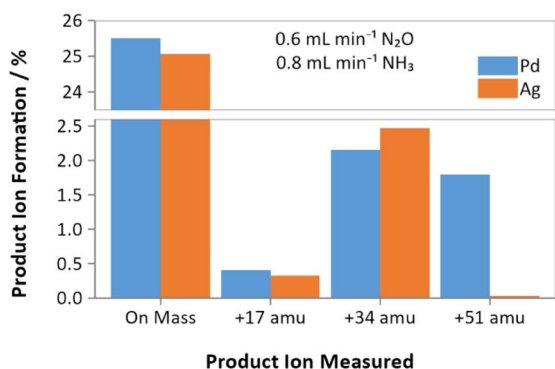


Fig. 7 Product ion formations of Pd (blue) and Ag (orange) with 0.6 mL min⁻¹ N₂O and 0.8 mL min⁻¹ NH₃ applied as a reaction gas mixture.

Caesium-135/137

¹³⁵Cs ($t_{1/2} = 1.33 \times 10^6$ years) and ¹³⁷Cs ($t_{1/2} = 30.018$ years) are important fission products used for environmental monitoring. Specifically, ¹³⁵Cs/¹³⁷Cs ratios have been used as a forensic tool to identify sources of radioactive contamination, for example following the Fukushima nuclear disaster.¹⁶ ICP-MS/MS methodology is already established for this application, where N₂O has already been used as a cell gas to separate ¹³⁵Cs⁺ and ¹³⁷Cs⁺ from the stable isobaric interferences of ¹³⁵Ba⁺ and ¹³⁷Ba⁺ respectively.¹⁴⁻¹⁶ By this approach, Ba is mass-shifted and the Cs can be determined on-mass. Additionally, Magre *et al.*¹⁸ recently described the use of an N₂O/NH₃ gas mixture for the determination of ¹³⁵Cs/¹³⁷Cs ratios with improved interference removal. The authors noted a sensitivity of 110 000 cps (ng⁻¹ mL⁻¹) (equivalent to 1 500 000 cps (Bq g⁻¹)) for ¹³⁵Cs and 34 cps (Bq g⁻¹) for ¹³⁷Cs) under wet-plasma conditions, with a factor of 3 times improvement using an Apex Ω desolvating system. The authors reported instrument blank levels of <0.6 cps. Under optimum conditions, including the use of the desolvating system, the authors achieved detection limits of 1.66 fg g⁻¹ (1.2 × 10⁻⁷ Bq g⁻¹) for ¹³⁵Cs and 0.67 fg g⁻¹ (0.0022 Bq g⁻¹) for ¹³⁷Cs.

The N₂O/NH₃ gas mixture was applied to the separation of Cs radionuclides from isobaric Ba interferences. At cell gas flow rates of 1 mL min⁻¹ N₂O and 0.1 mL min⁻¹ NH₃, separation factors of 223 000 for ¹³⁵Cs/¹³⁵Ba and 131 000 for ¹³⁷Cs/¹³⁷Ba were obtained, with sensitivities of 101 000 cps (ng⁻¹ g⁻¹) for both radioisotopes (Table S9) (equivalent to 1 370 000 cps (Bq g⁻¹) for ¹³⁵Cs and 31.4 cps (Bq g⁻¹) for ¹³⁷Cs). The instrument blank was found to be 0.7 cps for both ¹³⁵Cs and ¹³⁷Cs. The instrument detection limit under these conditions was calculated to be 0.017 pg g⁻¹ (equivalent to 1.3 × 10⁻⁶ Bq g⁻¹ for ¹³⁵Cs and 0.056 Bq g⁻¹ for ¹³⁷Cs). Compared to the use of N₂O only (optimum flow rate = 1 mL min⁻¹), the N₂O/NH₃ provided a factor of 2 times greater interference separation, while maintaining an equivalent sensitivity. Given the achieved sensitivity and blank levels, the results in this study are in good agreement with those produced by Magre *et al.*,¹⁸ though with higher observed detection limits due to the absence of a desolvating system.

Conclusions

This study demonstrates the promising applicability of N₂O for the removal of isobaric interferences for radionuclides of interest in nuclear decommissioning, especially for ⁶³Ni, ⁷⁹Se, and ⁹³Mo. Moreover, the great power of combining two reactive cell gases to open new interference removal pathways using new product ions is highlighted. In particular, enhanced interference removal for the group 2 radionuclides (⁴¹Ca and ⁹⁰Sr), as well as for ⁷⁹Se, ⁹³Mo, and ¹⁰⁷Pd were achieved using a novel N₂O/NH₃ gas mixture approach. Hence, it can be recommended that both N₂O and NH₃ are employed during ICP-MS/MS analysis. Such findings may also be applicable to stable isotope analysis, therefore further investigation is required into the use of the N₂O/NH₃ gas



mixture, as well as for other reactive cell gas mixtures, for a larger set of elements and additional radionuclides of interest, such as the actinides.

Author contributions

Shaun T. Lancaster: conceptualization, investigation, writing – original draft. Ben Russel: conceptualization, writing – review and editing. Thomas Prohaska: resources, writing – review and editing. Johanna Irrgeher: funding acquisition, resources, writing – review and editing.

Conflicts of interest

There are no conflicts to declare.

Data availability

The data supporting this article have been included as part of the SI. See DOI: <https://doi.org/10.1039/d5ja00254k>.

Acknowledgements

The project (21GRD09 MetroPOEM) has received funding from the European Partnership on Metrology, co-financed from the European Union's Horizon Europe Research and Innovation Programme and by the Participating States. The authors thank Karl Andreas Jensen, Solutions 4 Science, and PerkinElmer for fruitful discussions and continuous support.

Notes and references

- 1 I. W. Croudace, B. C. Russell and P. W. Warwick, *J. Anal. At. Spectrom.*, 2017, **32**, 494–526.
- 2 X. Hou and P. Roos, *Anal. Chim. Acta*, 2008, **608**, 105–139.
- 3 D. W. Koppenaal, G. C. Eiden and C. J. Barinaga, *J. Anal. At. Spectrom.*, 2004, **19**, 561–570.
- 4 L. Balcaen, E. Bolea-Fernandez, M. Resano and F. Vanhaecke, *Anal. Chim. Acta*, 2015, **894**, 7–19.
- 5 P. E. Warwick, B. C. Russell, I. W. Croudace and J. Zacharuskas, *Anal. At. Spectrom.*, 2019, **34**, 1810–1821.
- 6 S. Diez-Fernández, H. Isnard, A. Nonell, C. Bresson and F. Chartier, *J. Anal. At. Spectrom.*, 2020, **35**, 2793–2819.
- 7 D. J. Douglas and C. J. B. French, *J. Am. Soc. Mass Spectrom.*, 1992, **3**, 398–408.
- 8 D. J. Douglas, *J. Am. Soc. Mass Spectrom.*, 1998, **9**, 101–113.
- 9 P. Petrov, B. Russell, D. N. Douglas and H. Goenaga-Infante, *Anal. Bioanal. Chem.*, 2018, **410**, 1029–1037.
- 10 G. K. Koyanagi and D. K. Bohme, *J. Phys. Chem. A*, 2001, **105**, 8964–8968.
- 11 V. V. Lavrov, V. Blagojevic, G. K. Koyanagi, G. Orlova and D. K. Bohme, *J. Phys. Chem. A*, 2004, **108**, 5610–5624.
- 12 K. Harouaka, C. Allen, E. Bylaska, R. M. Cox, G. C. Eiden, M. L. di Vacri, E. W. Hoppe and I. J. Arnquist, *Spectrochim. Acta, Part B*, 2021, **186**, 106309.
- 13 S. T. Lancaster, T. Prohaska and J. Irrgeher, *J. Anal. At. Spectrom.*, 2023, **38**, 1135–1145.
- 14 M. Granet, A. Nonell, G. Favre, F. Chartier, H. Isnard, J. Moureau, C. Caussignac and B. Tran, *Spectrochim. Acta, Part B*, 2008, **63**, 1309–1314.
- 15 J. Zheng, W. Bu, K. Tagami, Y. Shikamori, K. Nakano, S. Uchida and N. Ishii, *Anal. Chem.*, 2014, **86**, 7103–7110.
- 16 T. Ohno and Y. Muramatsu, *J. Anal. At. Spectrom.*, 2014, **29**, 347–351.
- 17 K. J. Hogmalm, T. Zack, A. K. O. Karlsson, A. S. L. Sjöqvist and D. Garbe-Schönberg, *J. Anal. At. Spectrom.*, 2017, **32**, 305–313.
- 18 A. Magre, B. Boulet, H. Isnard, S. Mialle, O. Evrard and L. Pourcelot, *Anal. Chem.*, 2023, **95**, 6923–6930.
- 19 *Decay Data Evaluation Project*, http://www.lnhb.fr/home/conferences-publications/ddep_wg/.
- 20 J. Meija, T. B. Coplen, M. Berglund, W. A. Brand, P. De Bièvre, M. Gröning, N. E. Holden, J. Irrgeher, R. D. Loss, T. Walczyk and T. Prohaska, *Pure Appl. Chem.*, 2016, **88**, 293–306.
- 21 X. Hou, *Radiochim. Acta*, 2005, **93**, 611–617.
- 22 P. E. Warwick, I. W. Croudace and D. J. Hillegonds, *Anal. Chem.*, 2009, **81**, 1901–1906.
- 23 D. Hampe, B. Gleisberg, S. Akhmadaliev, G. Rugel and S. Merchel, *J. Radioanal. Nucl. Chem.*, 2013, **296**, 617–624.
- 24 B. Russell, H. Mohamud, M. G. Miranda, P. Ivanov, H. Thompkins, J. Scott, P. Keen and S. Goddard, *J. Anal. At. Spectrom.*, 2021, **36**, 845–855.
- 25 S. T. Lancaster, T. Prohaska and J. Irrgeher, *Anal. Bioanal. Chem.*, 2022, **414**, 7495–7502.
- 26 D. R. Bandura, V. I. Baranov, A. E. Litherland and S. D. Tanner, *Int. J. Mass Spectrom.*, 2006, **255–256**, 312–327.
- 27 X. Hou, L. F. Østergaard and S. P. Nielsen, *Anal. Chim. Acta*, 2005, **535**, 297–307.
- 28 P. E. Warwick and I. W. Croudace, *Anal. Chim. Acta*, 2006, **567**, 277–285.
- 29 I. Gresits and S. Tölgyesi, *J. Radioanal. Nucl. Chem.*, 2003, **258**, 107–112.
- 30 B. Russell, S. L. Goddard, H. Mohamud, O. Pearson, Y. Zhang, H. Thompkins and R. J. C. Brown, *J. Anal. At. Spectrom.*, 2021, **36**, 2704–2714.
- 31 N. Sugiyama and K. Nakano, *Reaction Data for 70 Elements Using O₂, NH₃ and H₂ Gases with the Agilent 8800 Triple Quadrupole ICP-MS*, Agilent Technical Note, 2014, P/N:5990-4585EN, https://www.agilent.com/cs/library/technicaloverviews/public/5991-4585EN_TechNote8800_ICP-QQQ_reactiondata.pdf.
- 32 I. M. Banjarnahor, V.-K. Do, T. Furuse, Y. Ohta and K. Tanaka, *J. Radioanal. Nucl. Chem.*, 2025, **334**, 4997–5306.
- 33 S. D'Illo, N. Violante, C. Majorani and F. Petrucci, *Anal. Chim. Acta*, 2011, **698**, 6–13.
- 34 P. Xu, C. Ding, G. Yu and Z. Chen, *J. Radioanal. Nucl. Chem.*, 2022, **331**, 3269–3274.
- 35 B. Russell, M. García-Miranda and P. Ivanov, *Appl. Radiat. Isot.*, 2017, **126**, 35–39.
- 36 J. Feuerstein, S. F. Boulyga, P. Galler, G. Stinger and T. Prohaska, *J. Environ. Radioact.*, 2008, **99**, 1764–1769.
- 37 Y. Luo, X. Hou, J. Qiao, L. Zhu, C. Zheng and M. Lin, *Anal. Chem.*, 2022, **94**, 11582–11590.



- 38 A. G. Espartero, J. A. Suárez, M. Rodríguez and G. Pia, *Appl. Radiat. Isot.*, 2002, **56**, 41–46.
- 39 S. Osváth, N. Vajda and Z. Molnár, *Appl. Radiat. Isot.*, 2008, **66**, 24–27.
- 40 A. Weller, T. Ramaker, F. Stäger, T. Blenke, M. Raiwa, I. Chyzhevsky, S. Kirieiev, S. Dubchak and G. Steinhauser, *Environ. Sci. Technol. Lett.*, 2021, **8**, 656–661.
- 41 M. Faure, C. Gautier, P. Fichet, A. Maubert, E. Debonnet, E. Laporte, C. Colin and L. Hélot, *J. Radioanal. Nucl. Chem.*, 2025, **334**, 4687–4707.

